On the use of Vibration Signal Analysis for Industrial Quality Control: Part II

Simone Delvecchio, Gianluca D'Elia, Marco Malagò and Giorgio Dalpiaz

Abstract Vibration signals can be successfully captured and analyzed for quality control at the end of the production line. Various signal processing techniques and their applications are presented in this paper. These applications demonstrate the importance of selecting proper signal processing tools in order to extract the most reliable information from the signals. The presented applications regards ball bearings and threshing process in harvesting machines.

Keywords Vibration · Condition monitoring · Diagnostics · Quality control · Ball bearings · Harvesting machines

1 Diagnostics of Distributed Faults in Ball Bearings

The study of localized failure detection in bearings started over two decades ago, embracing a large number of signal processing techniques that can be roughly subdivided with respect to their pertinence domain, i.e. time, frequency and time–frequency domain [1, 2]. The aim of this work is to apply cyclostationary metrics for the identification of both the appearance and the growth of distributed faults in ball bearings, in order to overcome the pitfall of the usual approaches. Non-

S. Delvecchio (✉) · G. D'Elia · M. Malagò · G. Dalpiaz
Engineering Department in Ferrara (EnDIF), University of Ferrara, Ferrara, Italy
e-mail: simone.delvecchio@unife.it

G. D'Elia
e-mail: gianluca.delia@unife.it

M. Malagò
e-mail: marco.malago@unife.it

G. Dalpiaz
e-mail: giorgio.dalpiaz@unife.it

G. Dalpiaz et al. (eds.), *Advances in Condition Monitoring of Machinery in Non-Stationary Operations*, Lecture Notes in Mechanical Engineering,
DOI: 10.1007/978-3-642-39348-8_35,

stationary signals can be defined as signals which satisfy a non-property, i.e. they do not satisfy the property of stationarity. It is not possible to define a general theory which treats non-stationary signals. The non-stationary behavior of each signal has to be individually evaluated [3–9]. An important cyclostationary tool is the Indicator of Second order cyclostationarity (ICS_{2x}) outlined in [10]. This indicator tries to quantify the distance of a second-order cyclostationary process from the closest stationary process having a similar power spectral density, giving an indication of the presence of second-order cyclostationary components within a signal. It is defined as (11):

$$ICS_{2x} = \sum_{\alpha \in A} \frac{\left| \left(\lim_{T \to \infty} \int_T |x^R(t)|^2 e^{-j2\pi\alpha t} dt \right) e^{2\pi\alpha t} \right|}{\lim_{T \to \infty} \int_T |x^R(t)|^2 dt} \tag{1}$$

where A is the set of all possible cyclic frequencies α and $x^R(t)$ is the residual signal. As reported by [10] this is a cumulant based estimator.

An experimental campaign was carried out on a ball bearing in order to obtain distributed faults on the outer race, by using a test-bed composed of an asynchronous 4-pole motor which moves a shaft by means of a driving belt. The shaft is supported by a couple of cone-shaped bearings, Fig. 1a. The bearing under test is a double-row self-aligning type SKF 1205; it is cantilever mounted on this shaft at the opposite to the pulley. A radial external load supplied by a leverage system acts on the test bearing. In the present test, the bearing was externally loaded with a force of 1962 N, while the shaft was rotating at 26.6 Hz. The bearing was degreased in advance in order to accelerate the wear process and then mounted on the test machine. Three accelerometers were used to measure the vibration signal. The vibration signals were acquired each 15 min with an acquisition time of 2 min, obtaining 21 acquisitions in total. The sampling frequency was 51.2 kHz. At the end of the test the bearing was unmounted to check the status of the

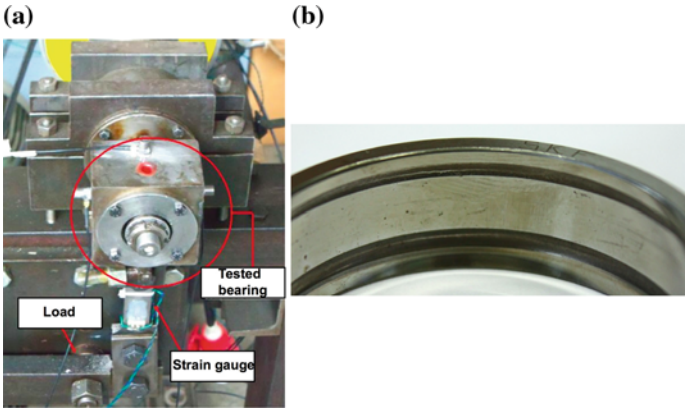

Fig. 1 **a** Test rig; **b** Bearing outer race at the end of the test

Table 1 Characteristic fault frequencies

Description	Symbol	[Hz]
Rotation frequency	*fr*	26.6
Outer race fault frequency	*fo*	127
Inner race fault frequency	*fi*	192
Cage fault frequency	*fc*	10.6
Ball fault frequency	*fb*	121

surfaces. The outer race of the bearing presented a groove corresponding to the passage of the balls, see Fig. 1b. The groove length took more or less half of the outer race circumference. The expected frequencies of the typical faults are computed from the usual formulae [11]. Their values for the bearing under test are collected in Table 1. Since the damage mainly involves the outer race in the actual case, the outer race fault frequency is briefly referred as "fault frequency" in the following.

In this paper it is considered only one of the three acceleration signals: it deals with the vibration signal that has be proven to be less affected by the transmission path. Figure 2 depicts the time signal captured during acquisitions n. 1 (first) and 21 (last) for a complete revolution of the shaft. As expected, the overall amplitude level strongly increases from the first to the last acquisition, but no impulsive content can be observed. Actually a distributed fault is not related to an impulsive content, but to an increase of the signal energy. Therefore, the evaluation of the RMS value can be an useful parameter for condition monitoring. As depicted in Fig. 3 the RMS value gives an alarm on acquisition 5 where probably the condition of the bearing is changed. However the RMS remains high until the end of the acquisitions giving no information about the evolution of the fault. In addition, due to its global nature, the RMS cannot give any information about the fault position. In order to better investigate the fault behavior, the classical envelope analysis is carried out by following these steps:

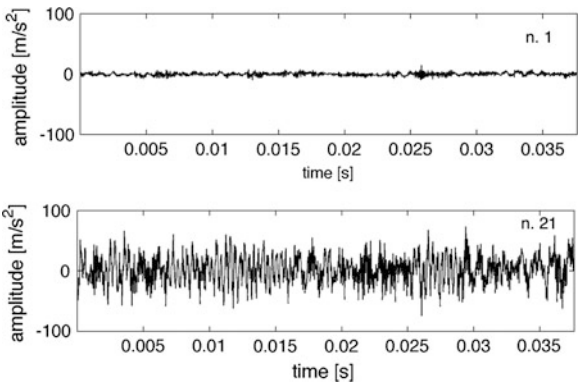

Fig. 2 Time signal for one shaft rotation: n. 1 first acquisition; n. 21 last acquisition

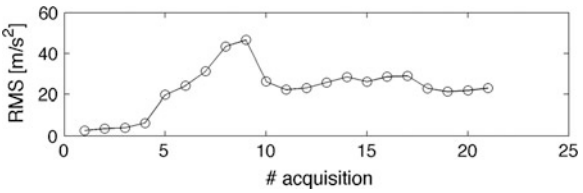

Fig. 3 RMS trend for acquisitions 1–21

- Band-pass filtering around a suitable frequency;
- Computation of the analytical signal, which is a complex quantity having the acquired signal as real part and its Hilbert Transform as imaginary part;
- Computation of the Spectrum of the absolute value of the analytical signal.

It can be noted that the envelope analysis (Fig. 4) confirms what found by the RMS value analysis trend. Moreover the envelope can identify the presence of a localized fault on the outer race around acquisition n. 5. In more details this localized fault gives origin to very slight but detectable impacts. The envelope is sensitive to these impacts showing the ball passing frequency on the incipient localized defect. Unfortunately this technique cannot supply further information concerning the increase of severity and extension of the wear. As a matter of fact, when the localized defect on the outer race grows, becoming a distributed fault, no impulses are generated; thus, this technique cannot highlight the fault evolution.

At this stage the cyclostationarity analysis [12] has been applied as a powerful tool in order to obtain information concerning the fault evolution. This type of analysis is well suited in describing the vibration response signal captured from a ball-bearing with a distributed fault. In fact, it is reasonable that this signal has non-stationary properties with a second-order cyclostationary content, due to the periodic variation of the bearing configuration. For example, the action of the balls passing on a distributed fault on the outer race produces a cyclostationary vibration with fundamental cyclic frequency corresponding to the ball passing frequency. The ICS_{2x} is evaluated in order to have a simple cyclostationary metric that can track the fault evolution. In particular, this metric is computed in the cyclic frequency range covering the first two fault harmonics. Figure 5 depicts the trend of this cyclostationary metric for all the acquisitions: this metric highlights both the fault appearance and the growth.

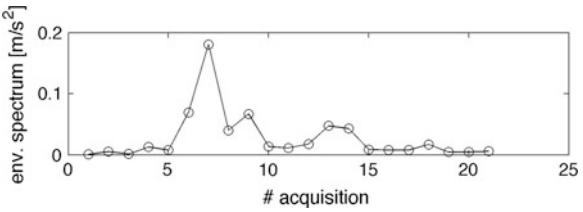

Fig. 4 Amplitude of the fault frequency component in the envelope spectrum of the raw signal: trend for acquisitions 1–21

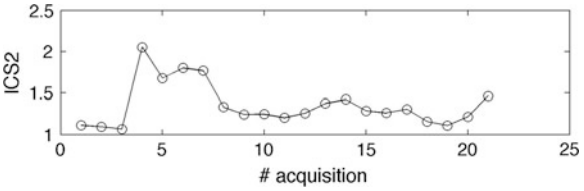

Fig. 5 *ICS2x* trend for acquisitions 1–21

2 Condition Monitoring of the Threshing Process in Harvesting Machines

This section of the paper concerns the analysis of the relationship between the threshing process in an axial flow harvesting machine and its vibro-acoustic behaviour. Several indoor and outdoor measurements are performed in various operational conditions in order to evaluate their influence on the vibration response of the threshing unit. The main goal was to identify a possible link between sound/vibration and crop distribution in threshing machines by using different signal processing tools.

The combine harvesting machine is a machine which "combines" the tasks of harvesting, threshing and cleaning grain plants. The desired result is the seed or grain (including corn, soybeans, flax, oats, wheat, or rye among others). In an axial combine harvester, as the crop spirals around the rotor, rasp bars mounted on the rotor rub the grains out. An helicoidally flux of the crop is favoured by splitting the incoming crop flow over two counter-rotating rotors. The threshing process is mainly given by two principal effects: (1) the "grain over grain" effect (i.e. the threshing of the grain kernels among themselves); (2) the threshing between kernels and concave (i.e. the rotor cage). The crop processing unit of an axial flow harvesting machine performs the following operations (Fig. 6): (1) after cutting the crop the threshing unit performs the threshing and separation activities making the kernels free from chaff and straw; (2) the cleaning unit cleans the crop separating the kernels from other small particles like chaff and short straw. The first operations are performed by the rotors that induce an helicoidal flux of the crop. Spirally arranged rasp bars and friction elements mounted on the rotors favor the friction of the crop against the concaves. There are four concaves, two for each rotor. The concave size, the number as well as the shape of the rasp bars changes as they go from the threshing zone to the separation zone.

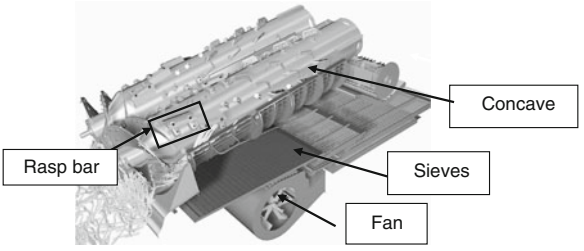

Fig. 6 Threshing unit: mechanical parts involved in the threshing process

The frequency analysis was firstly carried out for signals measured by 3 concave accelerometers in the radial direction. This direction was expected to be the most excited by the threshing flow. The middle signal presents higher amplitudes than the other signals from the front and rear concave accelerometers since they are mounted close to the bolt joints connecting the concave to the frame. The change in amount of crop processed between the concave front (beginning of the threshing zone) and rear positions (end of the threshing zone and start of the separation zone) does not affect the frequency behaviour, which is the same in the first 600 Hz for both positions. Thus, it is proven that the signal amplitudes are strongly dependent on the transducer location and not on the change of the amount of processed crop between the two positions. The relevant characteristic frequencies is supposed to be determined by the periodical rasp bar interactions of the rasp bars with the concave. Because of their helicoidally placement along the rotor, one rasp bar interacts with the concave three times during each rotor revolution. Therefore, it is useful to define a characteristic frequency as F_{bar} that can be expressed in Hz as $F_{bar} = 3n_{rotor}/60$, where n_{rot} is the nominal rotor speed in rpm.

On the basis of the first measurements the radial direction signal of the accelerometer positioned on the concave middle could be considered as the best correlated with the threshing process and it can be taken as the reference for the condition monitoring procedure. Based on the frequency behaviour, this signal can be decomposed into three different components: a component measured in idle condition due to the vibration of the mechanical parts in operation; a sinusoidal component given by the superposition of the F_{bar} and its harmonics; and a broadband random component. It is worth noting that the broadband spectrum component holds the response of the concave to two vibration sources: turbulence due to the threshing flow and hits of the kernels impacting the concave. For this reason the noise must not to be neglected during the analysis but has to be considered as "operational" noise generated by the process itself. In order to evaluate the influence of the operational parameters some vibration metrics are extracted from the raw vibro-acoustic signals: Root Mean Square value (RMS) reflecting the signal energy; Crest Factor (CF), Temporal Kurtosis (TK) and Impulse Factor (IF) reflecting the level of signal peakness. In particular the correlations among acceleration features and concave distance have been reported here. Looking at Fig. 7a, b and c it can be observed a very good correlation existing between the energy of all concave accelerometer signals and the concave distance: as the concave distance increases the Av. RMS decreases in a less than linear way. This is true for all capacity settings tested. When capacity is set at 10 % higher values are obtained. Based on these results we are able to link the concave vibration to the concave distance. Through the evaluation of the Av. RMS trends we get an idea of the global vibration of the concave. The TK of the concave middle radial signal for both indoor and outdoor tests (but here plotted only for signals measured during outdoor tests, see Fig. 7d) presents also good correlations with the concave distance variations. An increase of the concave distance causes an increase of the TK. This behaviour is probably due to the changes in crop distribution: at higher

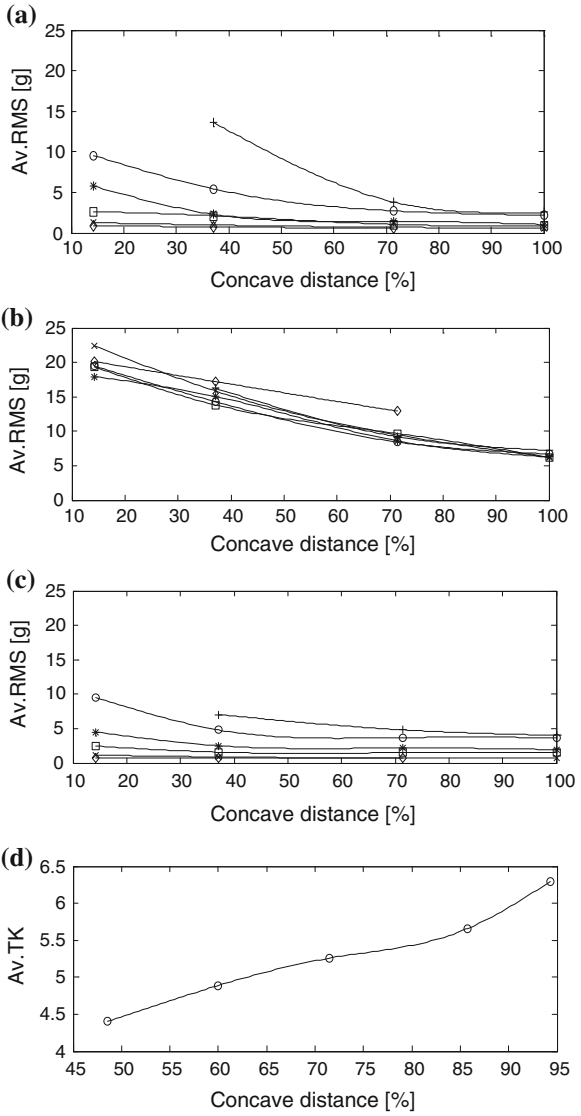

Fig. 7 Features versus concave distance: **a** Av. RMS at rear position; **b** Av. RMS at middle position; **c** Av. RMS at front position; **d** Outdoor tests: Av. TK at middle position

concave distances the crop is more spread less densely between the concave and the rotor. Therefore more space is available for the crop which interact more easily the concave. Hence we can refer to a sort of saturation effect occurring at low concave distances. Moreover, as confirmed by Fig. 8, it seems that the TK parameters can be correlated with the amount of broken grains. This correlation can be interpreted assuming that an increase of the concave distance, indicated by higher TK values, may cause a decrease in the impact force existing between the

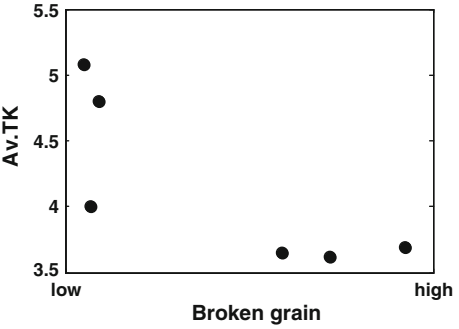

Fig. 8 Field tests: Av. TK versus broken grains

kernels and the concave giving a low percentage of broken grains. This phenomenon has to be investigated more in detail by further tests.

3 Concluding Remarks

This paper describes some applications of vibration analyses for the quality control of mechanical devices at the end of the production line.

A cyclostationary approach in order to identify distributed faults in ball bearings is proposed. The effectiveness of this approach is assessed through an experimental test: a degreased bearing running under radial load developed accelerated wear, while the vibration signal is periodically captured during the bearing life in order to monitor its deterioration. Classical and cyclostationary techniques are then applied to the signals. The results indicate that the usual approach can detect the appearance of the fault but cannot track the successive growth. On the contrary, cyclostationary tools are able to detect both the appearance of a localized fault and its development in a distributed fault.

Regarding the application in harvesting machines, appropriate metrics have been extracted from the time domain signals in order to explain the mechanism of the noise and vibration generation during the threshing process. Some correlations between these features and some operational and efficiency parameters have been obtained with the aim of determining how the crop distribution is influenced by varying these parameters. In particular, good correlations have been obtained for the concave middle radial signal, calculating the trends of RMS and TK. Some of these metrics can be assumed as good indexes that predict the efficiency of the process. Moreover, the concave vibration has been proved to be well correlated with the concave distance that is tuneable by the user during the field operations.

Acknowledgments This work has been developed within the Advanced Mechanics Laboratory (MechLav) of Ferrara Technopole, realized through the contribution of Regione Emilia-Romagna—Assessorato Attività Produttive, Sviluppo Economico, Piano telematico—*POR-FESR* 2007-2013, Activity I.1.1.

References

1. Delvecchio S, D'Elia G, Mucchi E, Dalpiaz G (2010) Advanced signal processing tools for the vibratory surveillance of assembly faults in diesel engine cold tests. J Vib Acoust 132(2):021008–021010, ISSN: 1048-9002, doi:10.1115/1.4000807
2. Mucchi E, Vecchio A (2010) Acoustical signature analysis of a helicopter cabin in steady-state and run up operational conditions. Measurement 43:283–293
3. Mucchi E, Dalpiaz G, Fernàndez del Rincòn A (2010) Elasto-dynamic analysis of a gear pump. Part I: pressure distribution and gear eccentricity. Mech Syst Signal Process 24:2160–2179. doi:10.1016/j.ymssp.2010.02.003
4. Mucchi E, Dalpiaz G, Rivola A (2010) Elasto-dynamic analysis of a gear pump Part II: meshing phenomena and simulation results. Mech Syst Signal Process 24:2180–2197. doi:10.1016/j.ymssp.2010.02.004
5. Mucchi E, Dalpiaz G, Rivola A (2010) Dynamic behaviour of gear pumps: effect of variations in operational and design parameters. Meccanica 46(6):1191–1212
6. Mucchi E, D'Elia G, Dalpiaz G (2012) Simulation of the running in process in external gear pumps and experimental verification. Meccanica 47(3):621–637
7. Mucchi E, Di Gregorio R, Dalpiaz G (2013) Elastodynamic analysis of vibratory bowl feeders: Modeling and experimental validation. Mech Mach Theory 60:60–72
8. Pierro E, Mucchi E, Soria L, Vecchio A (2009) On the vibro-acoustic operational modal analysis of a helicopter cabin. Mech Syst Signal Process 23:1205–1217
9. Mucchi E (2012) Experimental evaluation of modal damping of automotive components in different boundary conditions. Meccanica 47(4):1035–1041
10. Raad A, Antoni J, Sidahmed M (2008) Indicators of cyclostationarity: theory and application to gear fault monitoring. IEEE Trans Power Delivery 22:574–587
11. McFadden PD, Smith JD (1984) Vibration monitoring of rolling element bearings by the high-frequency resonance technique. a review. Tribol Int 17:3–10
12. Antoni J (2009) Cyclostationary by examples. Mech Syst Signal Process 23:987–1036